Photosynthesis Research (2024) 159:241–251
https://doi.org/10.1007/s11120-023-01039-5

RESEARCH

# Effect of cationic antiseptics on fluorescent characteristics and electron transfer in cyanobacterial photosystem I complexes

**Vladimir Z. Paschenko[1] · Eugene P. Lukashev[1] · Mahir D. Mamedov[2] · Daniil A. Gvozdev[1] · Peter P. Knox[1]**

Received: 17 February 2023 / Accepted: 9 July 2023 / Published online: 22 July 2023


## Abstract

In this study, the effects of cationic antiseptics such as chlorhexidine, picloxidine, miramistin, and octenidine at concentrations up to 150 μM on fluorescence spectra and its lifetimes, as well as on light-induced electron transfer in protein-pigment complexes of photosystem I (PSI) isolated from cyanobacterium *Synechocystis* sp. PCC 6803 have been studied. In doing so, octenidine turned out to be the most "effective" in terms of its influence on the spectral and functional characteristics of PSI complexes. It has been shown that the rate of energy migration from short-wavelength forms of light-harvesting chlorophyll to long-wavelength ones slows down upon addition of octenidine to the PSI suspension. After photo-separation of charges between the primary electron donor $P_{700}$ and the terminal iron-sulfur center(s) $F_A/F_B$, the rate of forward electron transfer from $(F_A/F_B)^-$ to the external medium slows down while the rate of charge recombination between reduced $F_A/F_B{}^-$ and photooxidized $P_{700}{}^+$ increases. The paper considers the possible causes of the observed action of the antiseptic.

**Keywords** *Synechocystis* sp. PCC 6803 · Photosystem I · Antiseptic · Octenidine · Fluorescence spectra · Fluorescence kinetics · Electron transfer

## Introduction

At present, an additional aspect may appear in the general problem of environmental pollution. This is due to the increasing and practically uncontrolled use of various antiseptic substances by mankind. The COVID pandemic has also given a powerful impetus to their introduction into everyday life. Obviously, the study of the environmental consequences of such a comprehensive use of these agents, which has a detrimental effect on living systems, is an urgent task. In previous studies, we evaluated the possible impact of a number of cationic antiseptics used in micromolar concentrations on the functioning of the photosynthetic apparatus of various photosynthetic organisms, which are at the beginning of global processes that ensure the very existence of life on earth. We have shown that in the photosynthetic membranes (chromatophore vesicles) from purple non-sulfur bacteria, these antiseptics disrupt the efficient transfer of absorbed light energy from the peripheral light-harvesting LH2 complexes to the LH1-reaction center (RC) core complex and then to the RC (Strakhovskaya et al. 2021; Knox et al. 2022). It is known that photosynthetic RCs of purple bacteria are the evolutionary precursors of higher plants photosystem II (PSII). In doing so, PSII is also included as an integral part in the photosynthetic apparatus of oxygen-producing cyanobacteria (precursors of chloroplasts) and algae (Raymond and Blankenship 2004). Consequently, the massive ingress of antiseptics into the planet's water resources may have significant negative consequences for both aquatic photosynthetic and terrestrial photosynthetic organisms in the future. Accordingly, in Paschenko et al. (2023), we studied the effects of cationic antiseptics on the functioning of the PSII core complexes isolated from spinach. As for isolated and purified photosynthetic protein complexes, these antiseptics obviously affected the structure of the internal light-harvesting complexes (CP43 and CP47 subunits) and, as a result, transfer of light excitation energy to the RC in PSII core complexes. It was shown that the rate of steady-state oxygen evolution by these complexes also decreased

✉ Daniil A. Gvozdev
danil131054@mail.ru

[1] Biophysical Department, Faculty of Biology, M.V. Lomonosov Moscow State University, Leninskye Gory 1, Build. 12, Moscow, Russia 119234

[2] A.N. Belozersky Institute of Physico-Chemical Biology, Moscow State University, Leninskye Gory 1, Build. 40, Moscow, Russia 119992

several times (Paschenko et al. 2023). In this series of studies of the possible global consequences of exposure to cationic antiseptics released into the environment, their impact on the functioning of the second energy-converting transmembrane pigment-protein complex of cyanobacteria and higher plants, the photosynthetic apparatus of photosystem I (PSI), has so far remained unexplored. The composition of these two main phototransforming macromolecular complexes (PSI and PSII) differs significantly, including in the content of lipids—one of the potential targets of cationic antiseptics. According to Sheng et al. (2018), each monomer of the homodimeric system of such a complex includes 34 well-defined lipid molecules, which are essential for the interaction of core subunits. Thus, octenidine can obviously serve as an effective agent that destabilizes the initial state of the photosynthetic pigment-protein complex (Paschenko et al. 2023). At the same time, the core complex PSI of cyanobacteria contains only 4 lipid molecules per monomer (Fromme 2004). In this regard, it seemed important to continue similar studies in the case of type I reaction center complexes (PSI).

In thylakoid membranes of oxygen-evolving organisms (cyanobacteria, algae, higher plants), two large pigment-protein complexes (PSI and PSII) act sequentially as light-driven photo-oxidoreductases. In doing so, PSI is one of the most advanced photovoltaic devices due to the unique combination of numerous exceptional features, including its high quantum efficiency (nearly 100%), vectorial charge transfer, and stability (reviewed in Golbeck 2006; Teodor and Bruce 2020; Hippler and Nelson 2021). It catalyzes the light-induced electron transfer from reduced plastocyanin or cytochrome (cyt) $c_6$ at the lumenal side of the thylakoid membrane to ferredoxin, a [2Fe–2S] soluble protein at the stromal side. In prokaryotes and some eukaryotic algae under iron-deficient conditions, ferredoxin can be replaced by flavodoxin, a low molecular mass flavoprotein (Rogers 1987).

Monomeric cyanobacterial PSI complex with a molecular mass > 370 kDa contains 12 different polypeptides (Jordan et a1. 2001). In doing so, 6 chlorophyll (Chl) *a* molecules in the catalytic core of two integral PsaA/PsaB subunits are surrounded by 90 Chl *a* and 22 *β*-carotene molecules, which serve together as core antenna pigments. All these redox cofactors except terminal iron-sulfur clusters $F_A/F_B$ are located within core subunits in a pseudosymmetrical manner and form two (A and B) branches for potential electron transfer. The terminal electron acceptors $F_A$ and $F_B$ are associated with the extrinsic stromal subunit PsaC.

The absorption maximum of the primary PSI donor ($P_{700}$) is localized at about 700 nm, while the maximum of the absorption band of most Chl antenna molecules is located at ~ 680 nm. There is also a fraction of Chl molecules that has a longer absorption wavelength than $P_{700}$. These are the so-called red forms of Chls. They may be the result of exciton interaction between several Chl molecules and their subsequent mixing with charge transfer states (Szewczyk et al. 2017). It is possible that at least part of them is localized on the periphery of the PSI core. In PSI trimeric complexes, the number of red forms of Chl molecules is slightly higher than in PSI monomeric complex: ~ 4–5 versus ~ 3, respectively (Gobets et al. 2003).

Energy conversion process on picosecond time scale in PSI preparations from *Synechocystis* sp., reflecting the capture and transfer of light excitation energy, has been studied in many works (Hastings et al. 1994; Turconi et al. 1996; Gobets et al. 2001, 2003; El-Mohsnawy et al. 2010; Szewczyk et al. 2017). Despite differences in experimental techniques and sample preparation, the overall results obtained in these studies are similar. Usually, in the fluorescence decay kinetics, components with $\tau \approx 0.5$ ps, 4–7 ps, 20–50 ps, and a component of nanosecond lifetime are distinguished. The first two fastest components are attributed to the equilibration of the excitation energy between different spectral forms of Chl. A component with a lifetime of 20–50 ps a disappearance time of the spectrally equilibrated excited state due to capture by RCs while the third component is the fluorescence of disconnected chlorophyll-protein complexes. In this case, the general dynamics of excitation is similar in monomeric and trimeric PSI complexes, which obviously reflects the similarity in the efficiency of charge separation in these complexes. In addition, the recorded fluorescence kinetics does not change significantly depending on whether RCs are open or closed (Byrdin et al. 2000).

After light absorption, the excitation energy within the RC is transferred to the primary electron donor, $P_{700}$. The excited state of the latter is a trigger for rapid electron transfer to the terminal $F_A/F_B$ iron-sulfur centers through a series of low-potential electron acceptors, which include the primary chlorophyll acceptor $A_0$, a phylloquinone $A_1$, and the $F_X$, $F_A$, and $F_B$ iron-sulfur clusters (type 4Fe–4S). At each transfer step, the electron is stabilized against charge recombination for progressively longer times. Concurrently with that, photooxidized $P_{700}$ is subsequently reduced by native protein donor, cyt $c_6$, while reduced $F_A/F_B$ is oxidized by ferredoxin.

Note that the processes of charge separation in PSI reaction center between $P_{700}$ and the iron-sulfur center $F_X$ and further electron transfer to the terminal $F_A/F_B$ as well as re-reduction of $P_{700}^+$ by external electron donor(s) such as cyt $c_6$ or artificial redox mediators *N*,*N*,*N*′*N*′-tetramethyl-p-phenylenediamine (TMPD), or 2,6-dichlorophenolindophenol (DCPIP)—ascorbate redox couples are accompanied by generation of transmembrane electric potential difference. The latter can be detected using direct electrometrical technique under single turnover of PSI protein complex asymmetrically incorporated into liposomes (reviewed in Mamedov et al. 2010).

In the present work, we studied the effect of cationic antiseptics (mainly octenidine) on the fluorescence characteristics and electron transfer processes in PSI protein-pigment complexes isolated from the cyanobacterium *Synechocystis* sp. PCC 6803. The structures of octenidine dihydrochloride is shown below:

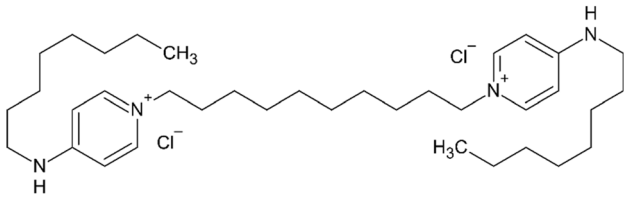


## Materials and methods

### Isolation and purification of PSI complexes

A glucose-tolerant wild-type strain of *Synechocystis* sp. PCC 6803 was grown at 30 °C in BG-11 medium with 5 mM glucose under light-activated heterotrophic growth conditions in the dark, as previously described (Anderson and McIntosh 1991). Thylakoid membranes were isolated according to Smart et al. (1991). PSI from cyanobacterium cells was prepared as described by Shen et al. (2002) with some minor modifications as outlined here. In brief, during solubilization, the thylakoid membranes were diluted to 0.5 mg Chl per ml in buffer (50 mM Hepes–NaOH, pH 7.5) and 1.0% n-dodecyl $\beta$-D-maltoside (DDM (w/v)) and solubilized for 2 h at 4 °C. The solution was clarified by centrifugation for 15 min at 14,000×*g*, and the supernatant was loaded onto a 5–20% (w/v) linear sucrose gradient prepared in 50 mM Hepes–NaOH (pH 8.0) buffer containing 0.03% (w/v) DDM. The gradients were centrifuged for 16 h at 140,000×*g*, using a SW 28 rotor and the lower, dark green band containing PSI complexes were collected. After concentration of fraction, the PSI complexes were twice dialyzed against 50 mM Hepes–NaOH (pH 7.5) buffer containing 0.03% (w/v) DDM for 2 h using a 50,000 molecular weight cut-off dialysis membrane. Fractions were collected and concentrated using Centricon-50 centrifugal concentrators (50-kDa cut-off membrane, Amicon, Beverly, MA). A stock PSI suspension (2 mg per $ml^{-1}$) in 50 mM Hepes buffer (pH 7.5) was frozen as small aliquots in liquid nitrogen, and stored at − 70 °C.

### Absorbance and fluorescence measurements

Absorption spectra were recorded using a modified Hitachi-557 spectrophotometer (Japan). Fluorescence spectra in the region 600–850 nm were recorded using a Fluorolog 3 spectrofluorometer (Horiba Jobin Yvon, Japan). Fluorescence was excited at the Soret absorption band (400 nm) of porphyrin pigments. Samples were prepared in 1 cm pathlength quartz cells with absorbance less than 0.1 unit to uniformly illuminate across the sample and to avoid the inner-filter effect. The dark counts were subtracted and the spectra were corrected for wavelength-dependent instrument sensitivity.

Fluorescence decay kinetics were recorded using photon counting at a wavelength of 680 nm with a Becker & Hickl (Germany) system in the time-correlated single photon counting (TCSPC) mode. This system provided instrumental response function (IRF) of the recording system of approximately 32 ps. A Tema-150 femtosecond laser system (Avesta Project, Russia) generated light pulses with a wavelength of 400 nm, duration of 300 fs, and repetition rate of 80 MHz (the average radiation power that was 2.8 W was used as an excitation light source; energy of a single laser pulse was 34 nJ). In our experiments, energy of the excitation light pulses was reduced by means of neutral light filters to a level determined by the sensitivity of the recording system; average radiation power density was 35 μW/$cm^2$. A three-exponential approximation was used to fit fluorescence kinetics. The measurements were repeated three times, and the mean values with standard error were used to calculate lifetime ($\tau$) and yield (F) of fluorescence.

Flash-induced absorption changes of PSI at 700 nm were examined by lab-made flash-photolysis system with double monochromatized probing light. Sample in 10 mm × 10 mm quartz cuvette was placed in Peltier-based thermostated holder Qpod-2e (Quantum Northwest, USA) set at temperature + 20 °C. Probing light (halogen lamp 12 V, 100 W, OSRAM, Germany) passes the first monochromator before sample and second one between sample and photomultiplier 9658B (Electron Tubes Ltd., UK). To protect the PMT from the fluorescence of the sample and the scattered light of the laser flash, a 700 nm interference optical filter with HBW of ~ 10 nm (Knight Optical, UK) was placed on the entrance slit of the second monochromator. The second harmonic of a 7 ns Nd-YAG Q-switched laser (LOTIS TII, Belarus) at 532 nm was used for photoexcitation. Energy of flashes was about 10 mJ/$cm^2$, far below the threshold that causes irreversible bleaching of the pigments and protein degradation. The duration between flashes was set at 5 s to allow completion of $P700^+$ dark reduction. Flash-induced absorbance changes in the 1 μs to 5 s time domain were digitized with a GaGe Octopus board (model CS8327, DynamicSignals, Canada). To achieve a higher signal-to-noise ratio, 50 single traces were averaged. The $8 \times 10^6$ data points collected were reductively averaged so as to provide 280 points on a logarithmic time scale. The kinetic traces were fit with a sum of exponentials using Mathematica (Wolfram Research,

USA) and OriginPro 9 (OriginLab, USA) software. The Chl concentration in the samples was ~ 15 µg/ml.

Because the isolated PSI complexes do not contain the natural cyt $c_6$ donor protein, in all experiments, 10 µM DCPIP and 5 mM sodium ascorbate have been added to the sample as an exogenous electron donor.

## Results and its discussion

### Effect of antiseptics on the fluorescent characteristics of PSI complexes

The absorption spectra of monomeric and trimeric complexes of PSI at room temperature practically coincide. There is a very small decrease in absorption at > 700 nm for monomeric form of PSI, related to a large absorption of red forms of Chl in trimeric complexes (Toporik et al. 2020). The fluorescence spectra of mono- and trimeric complexes of PSI preparations detected at room temperature are also very similar (Turconi et al. 1996). The obtained absorption and fluorescence spectra of the PSI complexes isolated from wild-type cyanobacterium *Synechocystis* sp. PCC6803 are shown in Fig. 1 (black curves).

They actually coincide with the spectra for PSI preparations described in the references (Turconi et al. 1996; Cherubin et al. 2019; Toporik et al. 2020). The main fluorescence maximum revealed in the spectrum and illustrated in the present work, as well as described in Cherubin et al. (2019) and Toporik et al. (2020) is localized at ≈ 684 nm. There is also a wide shoulder in the red region around ~ 730 nm. In doing so, the fluorescence spectra of monomeric and trimeric forms of PSI from cyanobacterium *T. elongates* measured at room temperature (El-Mohsnawy et al. 2010) and theoretically calculated PSI fluorescence spectra (Pishchalnikov et al. 2017) have a markedly different behaviors compared to spectra described in Turconi et al. (1996), Cherubin et al. (2019), and Toporik et al. (2020), namely with a shoulder of ~ 690 nm and a red-shifted main maximum. Note that the shoulder at ~ 690 nm for PSI monomeric complex is much more pronounced, possibly due to the effect of the detergent, which solubilizes the total large surfaces of monomers (El-Mohsnawy et al. 2010). In a number of studies (Cherubin et al. 2019; Toporik et al. 2020), it is not possible to understand whether the spectra presented in them refer to mono- or trimeric forms of PSI complexes. Turconi et al. (1996) have shown that the main maximum is shifted by a few nm to the short-wavelength side of the spectrum in the case of monomeric form of PSI. It should also be noted that the fluorescence of PSI preparations can be significantly affected by disconnected Chls that have lost their "native" interactions with the protein carrier. In doing so, their fluorescence maximum is localized at ≈ 675 nm (Szewczyk et al. 2017).

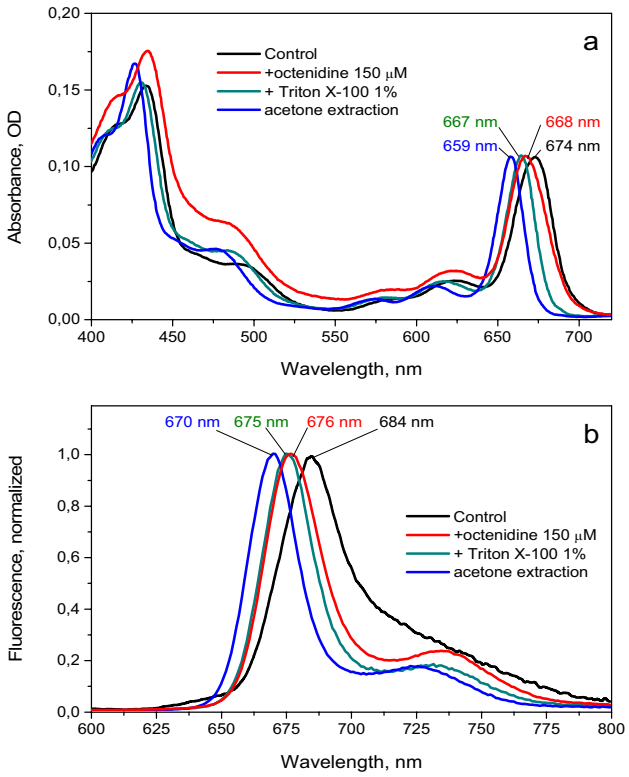


**Fig. 1** Absorption (**a**) and fluorescence (**b**) spectra of PSI complexes in control sample, and in the presence of octenidine at concentration of 150 µM, 1% Triton X-100, and in acetone-extracted solution. Fluorescence excitation at 400 nm

The fluorescence spectrum shown in Fig. 1B (black curve) allows us to conclude that it most likely represents a superposition of PSI mono- and trimeric forms.

We compared the effect of all four selected antiseptics at a concentration of 100 µM on PSI fluorescence spectrum and found that octenidine was several times more effective than the others. This is expressed both in a short-wavelength shift of the absorption spectrum maximum (Fig. 2), in an increase in fluorescence intensity as well as in a short-wavelength shift of the main fluorescence maximum (Fig. 3B and inset to Fig. 3B). In this study, therefore, the effect of octenidine on fluorescent characteristics and charge transfer in isolated PSI complexes has been studied in detail.

Analyzing the results, we can conclude that adding antiseptics probably has a certain effect on the stability of trimeric complexes of PSI. In addition, apparently, disconnected forms of Chl, which have a higher quantum yield of fluorescence, appear in proportion to the concentration of the added antiseptic. The result is shown in the Fig. 4, red circles.

Under our experimental conditions, when registering the fluorescence decay kinetics, the technique used with IRF ~ 32 ps does not allow us to resolve the fastest component in the decay kinetics described in the

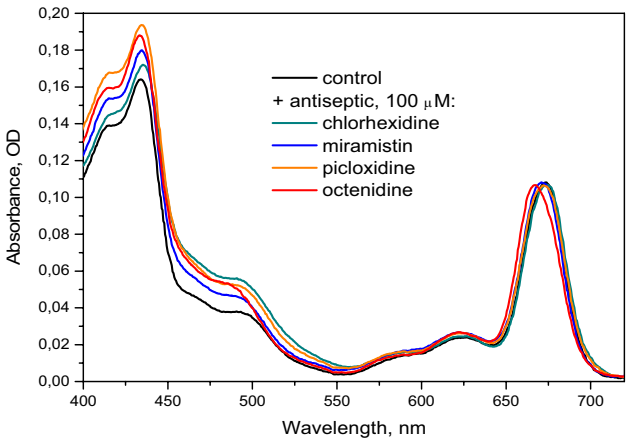


**Fig. 2** Normalized absorption spectra of PSI complexes in control sample and in the presence of 100 μM antiseptics

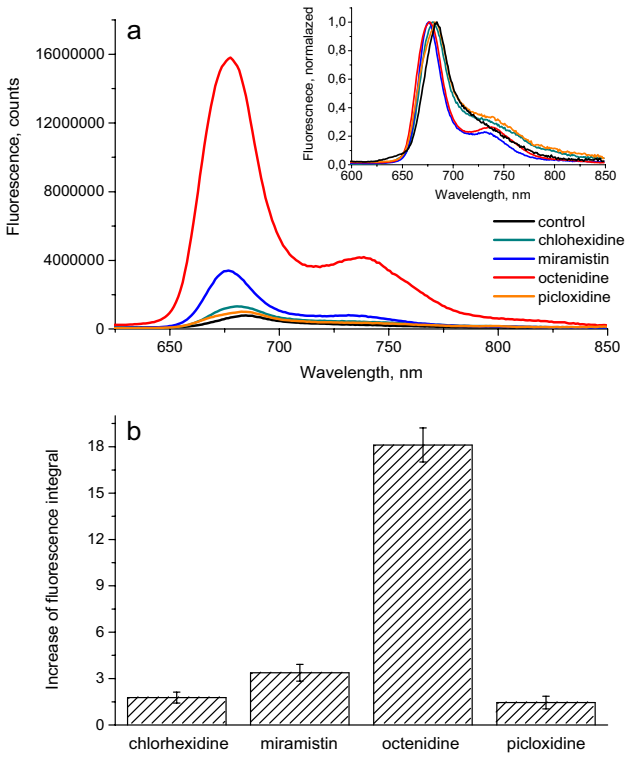


**Fig. 3** **a** Changes in fluorescence spectra of PSI complexes of control sample and in the presence of 100 μM antiseptics. Insert shows the normalized fluorescence spectra of the same samples. **b** Integral area of the main fluorescence band in PSI complexes upon addition of 100 μM antiseptics compared to the fluorescence of control sample (the area under the fluorescence curve for the control preparation was taken as unity). The measurements were repeated three times. The bar shows the standard deviation from mean value

literature: 4.8–5.0 ps (registered for monomeric complexes) or 6.7–7.1 ps (for trimeric PSI complexes) (Gobets et al. 2001). It is suggested that these fast components are due to

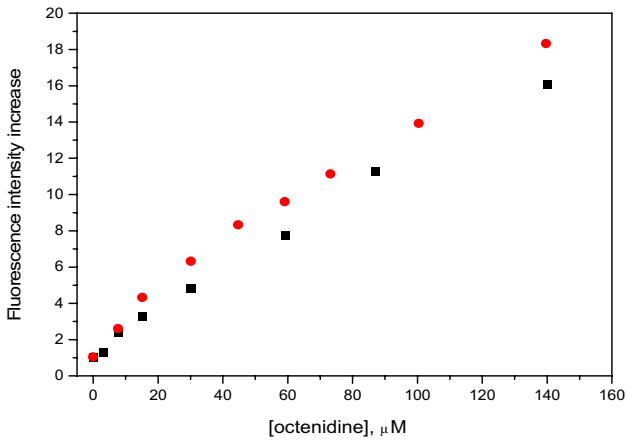


**Fig. 4** Change in the fluorescence quantum yield of PSI complexes determined by the ratio of the areas under the fluorescence curve (red circles) and by the areas under the fluorescence decay kinetics (black squares) on the concentration of octenidine

equilibration of the excitation energy between the bulk Chl and terminal emitter forms of Chl. The main contribution to the fluorescence decay kinetics in our measurements is made by a component with a lifetime of tens of ps, which is associated with the trapping time of excitation by the RC from these terminal emitter forms of Chl (Table 1). At the same time, the 3.4–15 ps components found by Gobets et al. (2001) were also attributed to the time of equilibration and localization of excitation on the terminal emitter forms of Chl. An obvious result of the action of antiseptics is the appearance of disconnected forms of Chl. The latter are characterized by fluorescence decay component in the ns time range (Gobets et al. 2001; Szewczyk et al. 2017).

In this work, we measured the fluorescence decay kinetics of control samples, as well as preparations at various concentrations of octenidine. The kinetic fitting results in the three-exponential approximation are presented in Table 1.

For control samples, the components of the fluorescence decay kinetics ($\tau_i$) were 63 ps, 0.51 ns, and 2.6 ns. The relative contribution of the two slowest phases was negligible, on the order of 2%. Note that since fluorescence kinetics measurements were carried out at one recording wavelength (at 680 nm), we failed to detect fastest components, described in previous work (Byrdin et al. 2000; Gobets et al. 2001), because we could not use the decay associated spectra method to reveal short-lived components.

The lifetime of the shortest-lived component $\tau_1 \approx 60$ ps (see Table 1) is determined by the efficiency of excitation energy capture by the PSI RC; its amplitude $a_1 = 95.7\%$ ($\sum a_i = 100\%$). Consequently, almost all Chl molecules of the PSI complex are active in terms of interaction (excitation energy transfer, EET) with RC. The longest-lived component of the fluorescence decay kinetics has a lifetime of $\tau_3 \approx 2.6$ ns and, according to the literature data (Byrdin et al.

**Table 1** The fluorescence lifetimes ($\tau_i$) and amplitude ($a_i$) for PSI complexes at different concentrations of octenidine

| | Control | 7.5 μM | 15 μM | 30 μM | 60 μM | 90 μM | 140 μM |
|---|---|---|---|---|---|---|---|
| $\tau_1$, ps | 63 ± 3 | 115 ± 6 | 166 ± 8 | 399 ± 15 | 602 ± 16 | 777 ± 18 | 922 ± 21 |
| $\tau_2$, ns | 0.51 ± 0.04 | 0.55 ± 0.06 | 3.1 ± 0.1 | 3.2 ± 0.1 | 4.2 ± 0.2 | 4.3 ± 0.2 | 4.8 ± 0.3 |
| $\tau_3$, ns | 2.6 ± 0.1 | 4.4 ± 0.2 | 5.1 ± 0.2 | 5.3 ± 0.1 | 5.5 ± 0.2 | 6.2 ± 0.2 | 6.2 ± 0.3 |
| $a_1$, % | 95.7 ± 4.4 | 70.0 ± 3.4 | 52.0 ± 3.1 | 26.7 ± 2.4 | 18.8 ± 1.7 | 14.1 ± 1.2 | 10.6 ± 1.4 |
| $a_2$, % | 2.6 ± 0.3 | 23.8 ± 0.9 | 30.2 ± 2.4 | 42.0 ± 4.1 | 60.8 ± 3.4 | 64.8 ± 4.2 | 66.9 ± 3.9 |
| $a_3$, % | 1.7 ± 0.2 | 6.2 ± 1.1 | 17.8 ± 2.1 | 31.3 ± 3.7 | 20.4 ± 2.0 | 21.1 ± 1.9 | 22.5 ± 2.4 |

$\lambda_{ex}$ = 400 nm, $\lambda_{reg}$ = 680 nm. The table shows the mean value for the three measurements and the standard error

2000; Gobets et al. 2001), refers to the uncoupled portion of antenna molecules not associated with RCs. From this, we can conclude that in the pigment-protein complexes of PSI in the absence of energy migration to RC, the fluorescence lifetime of light-harvesting Chl molecules is ~ 2.6 ns and the rate constant of intramolecular deactivation is $k_f + k_\Sigma = 4 \times 10^8$ $s^{-1}$. Here, $k_f$ is the emissive rate constant of Chl, $k_\Sigma$ is the sum of all nonradiative deactivation processes. Note that the amplitude of this component is insignificant and its value only 1.7%. In other words, only a few Chl molecules are in the uncoupled state in the control preparation. Finally, the second component with $\tau_2$ ~ 0.51 ns has an amplitude of 2.6%. We assume that this part of the Chl antenna molecules interacts both with the protein and partially with the RC. Previously, "the connectivity of PSII complexes in thylakoid membranes via electronically excited energy transfer, $k_{EET}$" has been proposed (Steffen et al. 2005). According to this conception, $k_{EET}$ is a structure-dependent factor and describes "the connectivity of the PSII RC complexes" in terms of energy transfer efficiency. Under limiting conditions, $k_{EET} = 1$ in the event of free excited energy transfer and $k_{EET} = 0$ for uncoupled pigment-protein complexes.

In our case, we will assume that for the vast majority of antenna molecules in PSI complexes, whose fluorescence lifetime is $\tau_1 = 63$ ps, the value of $k_{EET} = 1.0$, and for uncoupled Chl molecules, $k_{EET} = 0$. Then, for some of the molecules, whose fluorescence lifetime is $\tau_2 = 0.51$ ns, the factor $k_{EET} = 0.11$. Thus, it can be assumed that the light-harvesting pigments of photosynthetic organisms are involved in at least two types of interactions: (i) pigment–protein interactions of pigments with antenna structural proteins and (ii) interaction of pigment–protein complexes with RC complexes via excited energy transfer (factor of "connectivity").

When adding the most active antiseptic octenidine in increasing concentrations, the lifetime of the shortest component gradually increases from 63 to ~ 922 ps (Table 1). In this case, the amplitude of this component decreases from 95.7 to 10.6%. Two other components with lifetimes $\tau_2$ and $\tau_3$ behave differently. It can be seen (Table 1) that with an increase in the concentration of octenidine to 100 μM, $\tau_2$ increases from 0.51 to 4.8 ns, $\tau_3$ increases from ~ 2.6 to 6.2 ns. However, in contrast to the amplitude $a_1$, the amplitudes $a_2$ and $a_3$ increase from 2.6 to 66.9% ($a_2$) and from 1.7 to 22.5% ($a_3$). Such a change of the amplitudes of the components in the opposite direction indicates that under the action of octenidine, there is a decrease in the proportion of effectively interacting antenna Chls with RCs and a simultaneous increase in the proportion of weakly or not at all associated complexes with RCs. Thus, one of the targets of octenidine is the efficiency of antenna–RC interaction (connectivity $k_{EET}$).

An increase in $\tau_2$ and $\tau_3$ to ~ 5–6 ns (the value of $\tau_{fl}$ of free Chl) indicates that another target for octenidine is the efficiency of Chl-protein interactions. In other words, the bond between Chl molecules and the protein carrier in the antenna complexes weakens under the action of the antiseptic. As the concentration of the agent increases, the Chl molecules acquire the properties of free Chl.

It is important to note that the recorded increase in the quantum yield of PSI fluorescence in the presence of octenidine for the kinetics in experiments (calculated as areas under the kinetic curve—Fig. 4, black squares) is in good agreement for experiments on the measurement of steady-state fluorescence (calculated as areas under the fluorescence spectra—Fig. 4, red circles).

In our previous work (Paschenko et al. 2023), we showed that the action of the cationic antiseptic octenidine in spinach PSII core particles is generally similar to the action of the detergent Triton X-100. The addition of the latter also causes a short-wavelength shift of the absorption and fluorescence bands, an increase in the fluorescence quantum yield, as well as an increase in the lifetime to a value characteristic of free Chl. For PSI preparations, the effects observed were similar. Figure 1 shows the normalized absorption and fluorescence spectra of control preparations, as well as in the presence of octenidine, Triton X-100 and acetone. In the latter case, we have a solution of extracted Chl molecules. It can be seen that the absorption and fluorescence spectra of samples in the presence of octenidine and Triton X-100 are in good agreement, while the acetone treatment demonstrates a much greater short-wavelength shift of both the absorption maximum and the fluorescence one. However, based on

the lifetime, which for the sample in the presence of Triton X-100 at a concentration of 1% coincides with that for the acetone extract, the detergent completely monomerizes the PSI pigment apparatus. Some difference in the spectra is obviously a consequence of the preserved weak interaction of Chls with the protein matrix, which is completely lost in acetone. Figure 5 demonstrates the evolution of the kinetics of Chl fluorescence in PSI complex in the presence of octenidine—with an increase in its concentration, the kinetics approaches those characteristic of free monomeric Chl.

Inset to Fig. 5 depicts the IRF and the recorded fluorescence kinetics of PSI control samples on a picosecond time scale. It is clearly seen that the rise time of the intensity of the experimental kinetics is significantly longer than that of the IRF. In general, the excitation of terminal emitter forms of Chl, which fluoresce in the spectral region $\lambda_{reg} > 680$ nm, occurs both due to direct absorption of the excitation energy and due to energy migration from the short-wavelength forms of antenna Chl. According to Gobets et al. (2001), the terminal emitter forms are two antenna Chls, located ~ 14 Å from RC chlorophylls and form a structural and functional bridge between the other antenna Chls and RC. Based on the ratio of the number of short-wavelength and terminal Chl molecules (~ 90:2, Gobets et al. 2001), we can assume that the excitation of terminal molecules occurs mostly due to energy migration from short-wavelength forms of Chl. In this case, the rise of the acceptor fluorescence kinetics is determined by the lifetime of the excited state of the energy donor (Gvozdev et al. 2019). This is true for the case when the lifetime of the excited state of the donor is significantly less than the lifetime of the excited state of the acceptor. Based on these obvious considerations, we analyzed the effect of octenidine on the time of excitation energy equilibration in the PSI antenna complex. To do this, we measured the rise time of the fluorescence signal of the terminal emitter forms of Chl ($\lambda_{em} > 680$ nm) on the concentration of octenidine (Fig. 6A). It is seen from the Fig. 6B that the time of energy migration from short-wavelength forms to long-wavelength forms increases from 15 to 22 ps with the successive increase in the concentration of octenidine. Consequently, octenidine also affects the rate of excitation equilibration in the PSI antenna complex. Based on the value of the energy migration time (~ 15 ps; Fig. 6B of this paper and Gobets et al. 2001), we suggest that the energy transfer from short-wavelength forms of Chl ($\lambda_{fl} < 680$ nm) to terminal emitter forms ($\lambda_{fl} > 680$ nm) occurs via the Förster mechanism. Then, the reason for the slowdown in the rate of energy migration from short-wavelength forms of Chl to long-wavelength forms can be, for example, an increase in the value of the overlap integral and, possibly, the intermolecular distance, as well as a change in the mutual orientation of the dipole moments of transitions in the molecules of the energy donor and acceptor due to the disruption of Chl-protein interactions. As mentioned above, the weakening of such interactions with the addition of octenidine is the reason for the increase in the lifetime and fluorescence intensity of the samples, Table 1, Figs. 1, 4, 5.

## Effect of antiseptics on electron transfer in the PSI complex

We also studied the effect of octenidine on the process of dark reduction of photooxidized $P_{700}$ after activation of

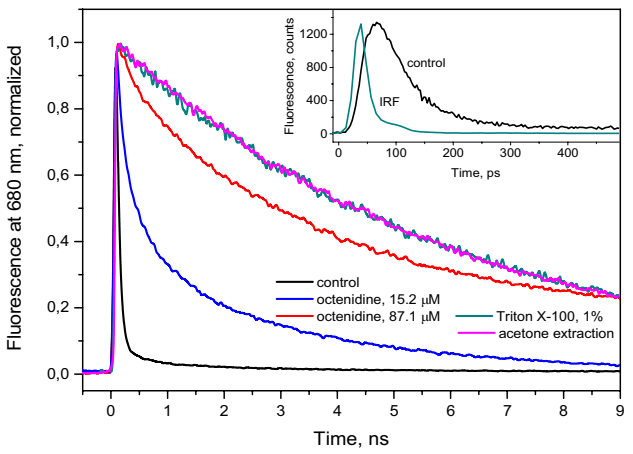


**Fig. 5** Fluorescence decay kinetics of PSI complexes in control sample, in the presence of octenidine, 1% Triton X-100 and in acetone-extracted solution. Inset shows the normalized IRF and fluorescence decay kinetics of control samples in picosecond time scale. $\lambda_{ex} = 400$ nm, $\lambda_{em} = 680$ nm

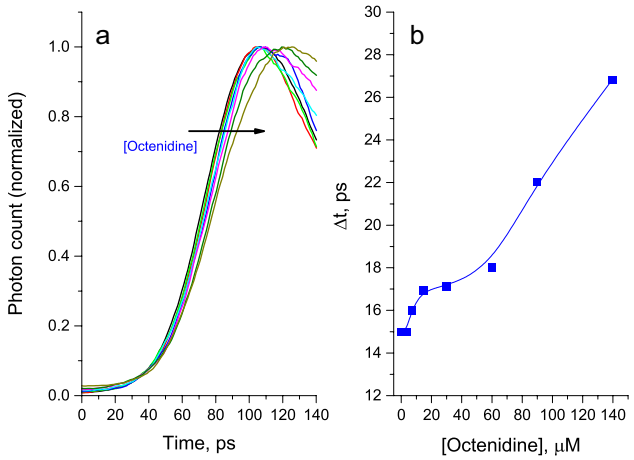


**Fig. 6** **a** Influence of octenidine on the rise time of fluorescence kinetics. The arrow in the figure shows the direction of increasing the duration of the rising edge of the fluorescence kinetics upon the successive addition of octenidine. **b** The time of equilibration of the excitation energy in the antenna complex of PSI at different concentrations of octenidine

preparations by single flashes of light. It is known that each PSI monomer has a core formed by the two largest subunits, PsaA and PsaB, which carry electron transport cofactors located in two symmetrical branches, A and B. Each branch starts from the Chl a $P_{700}$ dimer localized on the luminal side and ends with an iron-sulfur cluster [4Fe–4S] $F_X$ located on the opposite stromal side of the protein complex in the case of thylakoid membranes. Both branches are known to be active, but electron transfer along branch A is four times more efficient (Makita and Hasings 2015). Subsequently, the electron is transferred to the terminal $F_A/F_B$ clusters, which are associated with the peripheral PsaC protein subunit. If the electron transfer from the terminal $(F_A/F_B)^-$ cluster is further blocked, then the electron returns back to the oxidized $P_{700}^+$ within 30–100 ms. The recombination of electron between $P_{700}^+$ and the $F_X^-$ acceptor in the absence of the $F_A/F_B$ cluster occurs within 0.5–5 ms, while the recombination of $P_{700}^+$ with the primary acceptor $A_1^-$ (in the absence of all three iron-sulfur clusters) occurs within about 100 µs (Vassiliev et al. 1997). The thermodynamic and kinetic parameters of electron transfer in cyanobacterial PSI were considered in detail in (Milanovsky et al. 2017).

Figure 7 shows the kinetic curves of the dark reduction of $P_{700}^+$ in the control and in the presence of octenidine. Note that the PSI suspension used in this work contained DCPIP at a concentration of 10 µM and excess sodium ascorbate (5 mM) as an exogenous electron donor. The dark reduction kinetics of $P_{700}^+$ generally agrees well with that observed earlier on a similar cyanobacterial PSI preparation for the case of low excitation pulse intensity (Fig. 5 in Vasiliev et al. 1997). We did not observe any

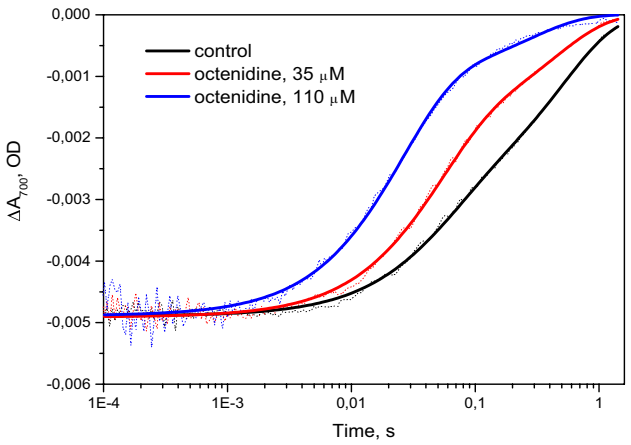


**Fig. 7** Kinetics of $\Delta A_{700}$ decay in PSI complexes in control sample and in samples in the presence of 35 µM and 110 µM octenidine. Points—experimental data, solid line—results of the two-exponential fit. The assay medium: 25 mM MES buffer (pH 7.0) containing 10 µM DCPIP and 5 mM sodium ascorbate. Excitation flash—532 nm, 7 ns, 10 mJ. Each curve is average of 50 traces acquired at 5 s intervals

changes in the amplitude of the induced $P_{700}^+$ signal in the time range from 2 µs to 1 ms after the flash. Based on the known literature data, it can be assumed that on a scale of tens hundreds of milliseconds, the photooxidized $P_{700}$ in the dark accepts an electron either as a result of back reaction from the terminal electron acceptor $(F_A/F_B)^-$ or from the exogenous donor DCPIP-$H_2$.

However, as the flash energy increased from 10 to 40 mJ, a microsecond phase appeared in the kinetics of $P_{700}^+$ reduction with τ about 200 µs and a very small contribution of about 2%. Such behavior of the reduction kinetics has been described previously (Vasiliev et al. 1997). Experimental data indicate that the fast recombination component reflects the interaction of photooxidized $P_{700}$ with the intermediate acceptor $(F_X)^-$, which is in the reduced state under the given conditions of light activation.

The reduction kinetics of $P_{700}^+$ in the control sample is fairly well approximated by two exponents with $\tau_1 \sim 50$ ms and an amplitude of ~ 37% and $\tau_2 \sim 500$ ms and an amplitude of ~ 63%. Note that the ~ 50 ms component probably reflects the reduction time of $P_{700}^+$ from $(F_A/F_B)^-$ while the 500 ms component reflects the reduction from the DCPIP-$H_2$ donor. Thus, the proposed scheme is as follows. After a flash of weak nonsaturating intensity, a certain distribution of electrons will be observed in the RC. In part of the RC, the electrons will be at the $(F_A/F_B)^-$, and in the other part, the electrons can move into the external medium to oxygen or the oxidized form of ascorbate, which are electron traps (Tributsin et al. 2014). In the latter case, $P_{700}^+$ will receive an electron from the excess DCPIP-$H_2$ at a rate an order of magnitude slower than from $(F_A/F_B)^-$ (~ 500 ms vs ~ 50 ms).

Since the forward electron transfer reactions are much faster than the back reactions, one can use a simple equation for calculating the population (α) from the electron population of the $F_A/F_B$:

$$\alpha = K_1/(K_1 + K_2),$$

where $K_1$ is the constant of back electron transfer from $(F_A/F_B)^-$ to $P_{700}^+$, and $K_2$ is the rate constant of electron transfer from $(F_A/F_B)^-$ into the bulk aqueous phase to oxygen or the oxidized form of ascorbate. Such a simplification is admissible, since the forward electron transfer constant from $(F_X)^-$ to $F_A/F_B$ is greater than the back electron transfer constant, and the reduction reaction constant from the DCPIP-$H_2$ is an order of magnitude smaller than the $K_1$ constant.

If we take the experimentally obtained values $\alpha = 0.37$ and $K_1 = 18.5$, then from the calculated value of the constant $K_2$, one can find the value $\tau = 32$ ms. It can be assumed that this value is the characteristic time of electron transfer from the terminal acceptor $(F_A/F_B)^-$ to the external medium.

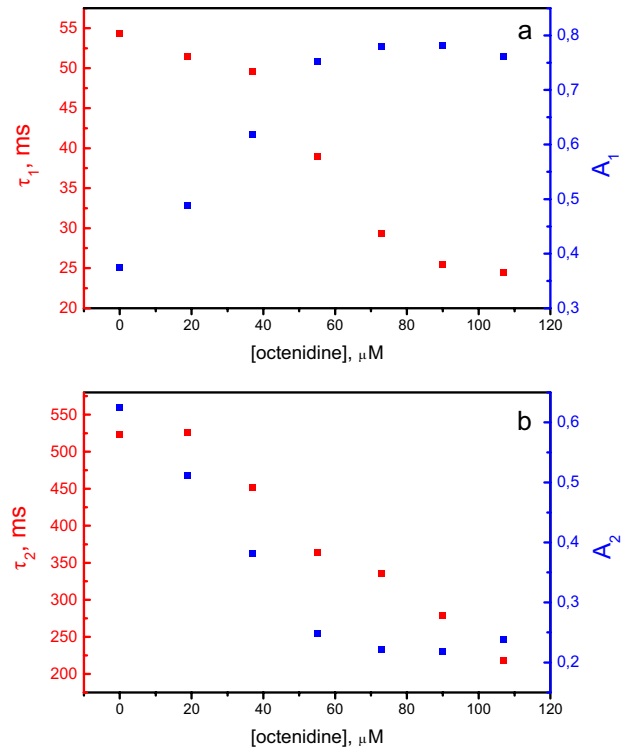


**Fig. 8** Results of the two-exponential fit of the $P_{700}^+$ decay kinetics at different octenidine concentrations. Panel **a** shows the parameters (amplitude $A_1$ and characteristic time $\tau_1$) of the fast reduction component reflecting the reverse electron transfer from the terminal cluster $(F_A/F_B)^-$. Panel **b** shows the corresponding parameters ($A_2$ and $\tau_2$) of the slow reduction component reflecting the delivery of the electron to $P_{700}^+$ from an exogenous donor

In the presence of octenidine, the $P_{700}^+$ reduction kinetics is also well described by two exponents. With an increase in the antiseptic concentration, the duration of the fast component decreases and its contribution increases, and the corresponding decrease in the contribution of the slow component occurs when its τ decreases. Figures 7 and 8 illustrate the change in these parameters with an increase in the concentration of the antiseptic in the medium. It should be noted that the main changes in kinetics occur up to an octenidine concentration of ~ 80 μM. With a further increase in the concentration of the antiseptic, the kinetics changes slightly.

Using the above formula, we find that at an octenidine concentration of 110 μM, the calculated electron transfer time from $(F_A/F_B)^-$ to the medium increases from 32 to 79 ms. Under these conditions, the back electron transfer reaction between $(F_A/F_B)^-$ and $P_{700}^+$ decreases from 54 to 25 ms (the amplitude increased from 0.37 to 0.76, and the time of the slow component decreased from 520 to 220 ms, with a corresponding decrease in the relative contribution). In other words, in the presence of octenidine, the electron from $(F_A/F_B)^-$ returns faster to $P_{700}^+$ and more slowly escapes into the environment. In doing so, the rate of $P_{700}^+$ reduction from an exogenous donor is more than doubles.

We do not know the exact mechanisms of the action of octenidine on the dark reduction of $P_{700}^+$, but it can be assumed that its properties as a surface-active compound are also manifested here. Loosening of the protein matrix not only disrupts the interaction between porphyrins, but also opens up greater access for the penetration of dye molecules (DCPIP-$H_2$) to the RC site on the lumenal side of PSI. This probably leads to an increase in the electron donation rate on $P_{700}^+$. At the same time, on the stromal side of PSI protein complex, disruption of electron stabilization at the terminal $F_A/F_B$ cluster can lead to an increase in the rate of charge recombination.

## Conclusion

The effects of the antiseptics octenidine, miramistin, chlorhexidine, and picloxidine on the spectral properties and energy migration processes have been previously investigated in chromatophore vesicles from non-sulfur purple bacteria *Rba. sphaeroides* and *R. rubrum* (Strakhovskaya et al. 2021; Knox et al. 2022), as well as in spinach PSII core complexes (Paschenko et al. 2023). Among these antiseptics, octenidine had the greatest influence on the above-mentioned characteristics of these photosynthetic preparations. It has been demonstrated that adding octenidine leads to an increase in the fluorescence intensity both in chromatophores and PSII core complexes by a factor of 5–10. It has been suggested that this effect is associated with a decrease in the rate constant of energy migration from LH2 to LH1 (*Rba. sphaeroides*) and from LH1 to the RC (*R. rubrum*). Similar spectral changes as well as decoupling between antenna complexes and RCs were observed in PSII core complexes. In addition, in PSII complexes under the action of octenidine, a decrease in the rate of oxygen evolution by 85% was observed compared with the control.

Similar effects were also observed in cyanobacterial PSI complexes in the presence of octenidine (present work): the fluorescence intensity increased by ~ 15 times, and the rate of energy transfer slowed down significantly. It has been suggested that octenidine affects two types of interactions: (i) interactions of Chl molecules with structural proteins and (ii) interactions of pigment–protein complexes with RC complexes via excited energy transfer (factor of connectivity, Steffen et al. 2005). Measurements of the fluorescence intensity rise time on the octenidine concentration reflect the rate of energy migration from the short-wavelength forms of the Chl antenna to the terminal emitter forms. We concluded that this antiseptic also affects the rate of excitation equilibration in the PSI antenna complex.

Finally, it was found that octenidine significantly affects the electron transfer rate in the PSI complex. Thus, at an octenidine concentration of 110 μM, the time of electron transfer from the $(F_A/F_B)^-$ to the external medium increases from 32 to 79 ms, while the rate of reverse (back) electron transfer from $(F_A/F_B)^-$ to $P_{700}^+$ decreases from 54 to 25 ms. In other words, in the presence of octenidine, an electron from terminal acceptor $(F_A/F_B)^-$ recombines twice as fast with $P_{700}^+$ and, accordingly, moves into the medium more slowly.

Let us briefly dwell on the possible "mechanisms" of the destructive action of cationic antiseptics on photosynthetic organisms. The action of antiseptics both on coupled membrane structures and on energy-converting protein complexes is obviously based on their amphiphilicity: the presence of simultaneously charged groups and hydrophobic tails. The maximum efficiency of the impact of octenidine, apparently, is due to the peculiarities of its structure. Octenidine [*N*,*N*′-(decane-1,10-diyldi-1(4H)-pyridyl-4-ylidene) bis(octylammonium) dichloride] belongs to the group of bispyridines, where the aminopyridine structure enables a mesomeric distribution of the cationic charge. The two cationic pyridine residues are separated by ten methylene groups, and each aminopyridine has a terminal hydrophobic octanyl group. In other words, the molecule is characterized by a pronounced amphipathic character, which allows it to be soluble in water and at the same time interacts with hydrophobic cell membranes, up to destruction of their structure (Malanovic et al. 2020). According to the results of this paper octenidine, with its positive charges, neutralizes the surface charge of the outer membrane of the bacterial cell. Because of hydrophobic interactions, the hydrocarbon chains from octenidine interfere with the fatty acyl chain region of the membrane core, inducing a complete lipid disorder based on hydrophobic mismatch. As a result, the introduction of octenidine into the membrane of bacteria leads to a chaotic arrangement of lipids and the rapid destruction of the cell membrane. The destruction of the normal structure of the model membrane upon interaction with octenidine was also demonstrated by the molecular dynamics method in the works (Kholina et al. 2020; Rzycki et al. 2021). The membranes of plant cells and chloroplasts differ in their lipid composition from the membranes of bacterial cells. But they also contain negatively charged and neutral lipids (see, for example, a review by Reszczyńska and Hanaka 2020). In other words, octenidine molecules, which have pronounced amphipathic properties, are likely to be able to interact with both the negatively charged surface of plant membranes and their hydrophobic acyl tails.

However, in the cyanobacterial PSI protein complex, the proportion of lipid molecules is low, only 4 molecules per monomer (Fromme 2004). Therefore, the consequences of the disaggregating action of octenidine on the lipid phase in these preparations obviously should not be decisive either. However, the amphiphilicity of the molecule allows it to interact effectively with PSI protein components. We have already discussed (see above) detergent-like properties of octenidine. The effects observed in the present work are probably due to the interaction of a pronounced amphiphilic octenidine molecule with amphiphilic surfaces in the protein subunits of the PSI complex. This leads both to disaggregation of light-harvesting Chl molecules bound to the protein matrix and to disruption of the integrity of the acceptor and donor sites of the RC electron transport chain.

Thus, summing up the results of our research cycle derived from various samples, one can suggest that octenidine has a strong effect on the processes of light energy conversion by the components of the photosynthetic apparatus of purple bacteria *Rba. sphaeroides* and *R. rubrum*, as well as PSII core complexes from spinach and PSI particles from cyanobacterium *Synechocystis* sp. PCC6803. The consequences of its use on a large scale can have a negative impact on the environment.

**Author contributions** Conceptualization: VZP, PPK.Methodology: EPL, MDM.Formal analysis and investigation: EPL, MDM, DAG. Writing—original draft preparation: MDM, PPK.Writing—review and editing: VZP, EPL, MDM, DAG, PPK.Supervision: VZP.

**Funding** Funding was provided by Science Project of the State Order of the Government of Russian Federation (121032500058-7).

## Declarations

**Competing interests** The authors declare no competing interests.

## References

Anderson SL, McIntosh L (1991) Partial conservation of the 5'*ndh*E-*psa*C-*ndh*D 3' gene arrangement of chloroplasts in the cyanobacterium *Synechocystis* sp. PCC 6803: implications for NDH-D function in cyanobacteria and chloroplasts. Plant MolBiol 16:487–499

Byrdin M, Rimke I, Schlodder E, Stehlik D, Roelofs TA (2000) Decay kinetics and quantum yields of fluorescence in photosystem I from *Synechococcus elongatus* with P700 in the reduced and oxidized state: are the kinetics of excited state decay traplimited or transferlimited? Biophys J 79:992–1007

Cherubin A, Destefanis L, Bovi M et al (2019) Encapsulation of photosystem I in organic microparticles increases its photochemical activity and stability for ex vivo photocatalysis. ACS Sustain Chem Eng 7:10435–10444

El-Mohsnawy E, Kopczak MJ, Schlodder E, Nowaczyk M, Meyer HE, Warscheid B, Karapetyan NV, Rogner M (2010) Structure and function of intact photosystem I monomers from the cyanobacterium *Thermosynechococcus elongatus*. Biochemistry 49:4740–4751

Fromme P (2004) Photosystem I, structure and function. Encyclopedia of biological chemistry, vol 3. Elsevier, Amsterdam, pp 342–347

Gobets B, van Stokkum IHM, Rögner M, Kruip J, Schlodder E, Karapetyan NV, Dekker JP, van Grondelle R (2001) Timeresolved fluorescence emission measurements of photosystem I particles of various cyanobacteria: a unified compartmental model. Biophys J 81:407–424

Gobets B, van Stokkum IHM, van Mourik F, Dekker JP, van Grondelle R (2003) Excitation wavelength dependence of the fluorescence kinetics in photosystem I particles from Synechocystis PCC 6803 and *Synechococcus elongatus*. Biophys J 85:3883–3898

Golbeck JH (ed) (2006) Photosystem I: the light-driven plastocyanin: ferredoxinoxidoreductase. Springer, New York

Gvozdev DA, Lukashev EP, Gorokhov VV, Paschenko VZ (2019) Photophysical properties of upconverted nanoparticles photocyanine complexes. Biochem Mosc 84:911–922

Hastings G, Kleinherenbrink AM, Lin S, Blankenship RE (1994) Timeresolved fluorescence and absorption spectroscopy of photosystem I. Biochemistry 33:3185–3192

Hippler M, Nelson N (2021) The plasticity of photosystem I. Plant Cell Physiol 62:1073–1081

Jordan P, Fromme P, Witt HT, Klukas O, Saenger W, Krauss N (2001) Three-dimensional structure of cyanobaoterial photosystem I at 2.5 Å resolution. Nature 411:909–917

Kholina EG, Kovalenko IB, Bozdaganyan ME, Strakhovskaya MG, Orekhov PS (2020) Cationic antiseptics facilitate pore formation in model bacterial membranes. J Phys Chem B 124:8593–8600

Knox PP, Lukashev EP, Korvatovskiy BN, Strakhovskaya MG, Makhneva ZK, Bol'shakov MA, Paschenko VZ (2022) Disproportionate effect of cationic antiseptics on the quantum yield and fuorescence lifetime of bacteriochlorophyll molecules in the LH1-RC complex of *R. rubrum* chromatophores. Photosynth Res 153:103–112

Makita H, Hasings G (2015) Directionality of electron transfer in cyanobacterial photosystem I at 298 and 77 K. FEBS Lett 289:1412–1417

Malanovic N, Ön A, Pabst G, Zellner A, Lohner K (2020) Octenidine: novel insights into the detailed killing mechanism of Gram-negative bacteria at a cellular and molecular level. Int J Antimicrob Agents 56:106146

Mamedov MD, Kurashov VD, Cherepanov DA, Semenov AYu (2010) Photosystem II: where does the light-induced voltage come from? Front Biosci 15:1007–1017

Milanovsky GE, Petrova AA, Cherepanov DA, Semenov AYu (2017) Kinetic modeling of electron transfer reactions in photosystem I complexes of various structures with substituted quinone acceptors. Photosynth Res 133:185–199

Paschenko VZ, Lukashev EP, Mamedov MD, Korvatovskiy BN, Knox PP (2023) Influence of the antiseptic octenidine on spectral characteristics and energy migration processes in photosystem II core complexes. Photosynth Res 155:93–105

Pishchalnikov RYu, Shubin VV, Razjivin AP (2017) Spectral differences between monomers and trimers of photosystem I depend on the interaction between peripheral chlorophylls of neighboring monomers in trimer. Phys Wave Phenom 25:185–195

Raymond J, Blankenship RE (2004) The evolutionary development of the protein complement of Photosystem 2. Biochim Biophys Acta 1655:133–139

Reszczyńska E, Hanaka A (2020) Lipids composition in plant membranes. Cell Biochem Biophys 78:401–414

Rogers LJ (1987) Ferredoxins, flavodoxins and related proteins: structure, function and evolution. In: Fay P, Van Baalen C (eds) The cyanobacteria. Elsevier, Amsterdam, pp 35–67

Rzycki M, Drabik D, Szostak-Paluch K, Hanus-Lorenz B, Kraszewski S (2021) Unraveling the mechanism of octenidine and chlorhexidine on membranes: does electrostatics matter? Biophys J 120:3392–3408

Shen G, Zhao J, Reimer SK, Antonkine ML, Cai Q, Weiland SM, Golbeck JH, Bryant DA (2002) Assembly of photosystem I. I. Inactivation of the rubA gene encoding a membrane associated rubredoxin in the cyanobacterium *Synechococcus* sp. PCC 7002 causes a loss of photosystem I activity. J Biol Chem 277:20343–20354

Sheng X, Liu X, Cao P, Li M, Liu Z (2018) Structural roles of lipid molecules in the assembly of plant PSII-LHCII supercomplex. Biophys Rep 4:189–203

Smart L, Anderson S, McIntosh L (1991) Targeted genetic inactivation of the photosystem I reaction center in the cyanobacterium *Synechocystis* sp. *PCC*-6803. EMBO J 10:3289–3296

Steffen R, Kelly AA, Huyer J, Dörmann P, Renger G (2005) Investigations on the reaction pattern of photosystem II in leaves from *Arabidopsis thaliana* wild type plants and mutants with genetically modified lipid content. Biochemistry 44:3134–3142

Strakhovskaya MG, Lukashev EP, Korvatovskiy BN, Kholina EG, Seifullina NKh, Knox PP, Paschenko VZ (2021) The effect of some antiseptic drugs on the energy transfer in chromatophore photosynthetic membranes of purple non-sulfur bacteria *Rhodobacter sphaeroides*. Photosynth Res 147:197–209

Szewczyk S, Giera W, D'Haene S, van Grondelle R, Gibasiewicz K (2017) Comparison of excitation energy transfer in cyanobacterial photosystem I in solution and immobilized on conducting glass. Photosynth Res 132:111–126

Teodor AH, Bruce BD (2020) Putting photosystem I to work: truly green energy. Trends Biotechnol 38:1329–1342

Toporik H, Khmelnitskiy A, Dobson Z, Riddle R, Williams D, Lin S, Jankowiak R, Mazor Y (2020) The structure of a red-shifted photosystem I reveals a red site in the core antenna. Nat Commun 11:5279

Tributsin BV, Mamedov MD, Semenov AYu, Tikhonov AN (2014) Interaction of ascorbate with photosystem I. Photosynth Res 122(215):231

Turconi S, Kruip J, Schweitzer G, Rögner M, Holzwarth AR (1996) A comparative fluorescence kinetics study of photosystem I monomers and trimers from *Synechocystis* PCC 6803. Photosynth Res 49:263–268

Vassiliev IR, Jung Y-S, Mamedov MD, Semenov AYu, Golbeck JH (1997) Near-IR absorbance changes and electrogenic reactions in the microsecond-to-second time domain in photosystem I. Biophys J 72:301–315